CHAPTER 280

Design Capacity of a Longshore Current Recirculation System for a Longshore Sediment Transport Laboratory Facility

David G. Hamilton[1], Julie D. Rosati[2], Jimmy E. Fowler[2], and Jane M. Smith[2]

ABSTRACT

A new longshore sediment transport laboratory facility for conducting three-dimensional moveable-bed experiments is being developed by the U.S. Army Engineer Waterways Experiment Station, Coastal and Hydraulics Laboratory. This paper focuses on the problem of designing the pumping capacity for an external longshore current recirculation system, designed to minimize adverse laboratory effects created by the updrift and downdrift lateral boundaries of the new facility. A review of longshore current recirculation systems used in other laboratory facilities is presented. The numerical model NMLONG is used to predict the magnitude and cross-shore distribution of the wave-driven longshore current that will be generated during experiments in the new facility. This paper concludes with a performance curve that defines the required pumping capacity of each of the individual pumps in the longshore current recirculation system.

1. INTRODUCTION

In performing its mission to maintain navigable waterways along U.S. coasts, the U.S. Army Corps of Engineers (USACE) regularly applies analytical and numerical models to estimate the total longshore sediment transport (LST) rate. Accurate prediction of LST rate is essential when predicting beach response in the vicinity of coastal structures, designing artificial beach nourishment projects, and approximating sedimentation rates in navigation channels. For design applications with adequate field measurements, the commonly used CERC formula (Shore Protection Manual, 1984) can be calibrated and applied to estimate total LST rates with reasonable confidence. However, for design applications without calibration data, the CERC formula provides only order-of-magnitude accuracy.

The present work is part of a research program intended to improve the USACE's capabilities to predict local and total LST rates and to evaluate errors associated with these predictions. The first goal of this research is to develop a world-class Longshore Sediment Transport Facility (LSTF) for conducting three-dimensional moveable-bed experiments. The LSTF will simulate nearshore hydrodynamic and sediment transport processes at a relatively large geometric scale. Further information on the objectives of this research program and general planning and design considerations for this new laboratory facility can be found in Rosati et al. (1995).

1 Coastal Engineer, CS-310 Cain Ridge Rd., Vicksburg, Mississippi, USA, 39180,
Tel: 601 634-3029, Fax: 601 634-4314, Email: D.Hamilton@CERC.WES.ARMY.MIL

2 Research Hydraulic Engineer, USAE Waterways Experiment Station, Coastal and Hydraulic Laboratory, 3909 Halls Ferry Road, Vicksburg, Mississippi, USA, 39180-6199

This paper focuses on the problem of calculating the required pumping capacity of a longshore current (LSC) recirculation system being designed to minimize the adverse laboratory effects created by the updrift and downdrift lateral boundaries of the LSTF.

The following sections review other LSC recirculation systems, provide a brief description of the LSTF, and discuss results obtained using the numerical model NMLONG to estimate the magnitude and cross-shore distribution of LSC that will be generated in the LSTF. Subsequent sections discuss limitations of the numerical analysis and other design parameters required to determine the design capacity of the LSC recirculation system. The final section provides a performance curve that defines the required pumping capacity for each of the individual pumps in the LSC recirculation system.

2. REVIEW OF OTHER LSC RECIRCULATION SYSTEMS

Early longshore current laboratory experiments were conducted without a LSC recirculation system that would have minimized the adverse laboratory effects created by the updrift and downdrift boundaries of each facility. Putman, Munk and Taylor (1949) used the sidewalls of the tank as wave guides to train the waves onto the beach. The LSC generated on the beach became part of the internal circulation pattern in the wave basin, which is considerably different then the situation on a long straight coast. Brebner and Kamphuis (1963) terminated the wave guides near the break point allowing the LSC to passively enter and exit the beach. Galvin and Eagleson (1965) and Mizuguchi and Horikawa (1978) terminated the downdrift wave guide at the break point, and completely closed the updrift wave guide. Apparently the longshore flux, in both of these experiments, was entering the test area underneath the wave generator, which would cause a non-uniform LSC distribution along the beach. Galvin and Eagleson (1965) were the first to measure the cross-shore distribution of LSC at several transects along the beach. Their data revealed the adverse effects created by the updrift and downdrift boundaries of the facility, in that the LSC was not able to reach its equilibrium magnitude and cross-shore distribution.

Visser (1982) conducted what appears to be the most detailed LSC experiments conducted to date. The wave basin was relatively large with a beach length between the wave guides of approximately 20 m. Visser's experiments were the first to use a LSC recirculation system to recirculate water from the downdrift to the updrift end of the beach. For most of Visser's experiments, the cross-shore distribution at the updrift boundary was controlled using 12 flow channels and control gates. Each flow channel was 0.2 and 0.4 m wide for tests with beach slopes of 1:10 and 1:20, respectively. Visser found it impossible to optimize the recirculation procedure from measurements of the mean water level in the longshore direction. He developed an alternative method where the optimum rate of external recirculation was determined by minimizing the internal circulation between the wave guides.

Simons et al. (1995) described some of the evaluation tests conducted in the recently developed Coastal Research Facility at HR Wallingford, in the United Kingdom. This facility was constructed in a large wave basin (27 x 54 m) and has a 36-m long directional wave generator. The most impressive component of the facility is the LSC recirculation system that has 4 independent reversible axial flow pumps with a total pumping capacity of

1.2 m^3/s. Currents are introduced into the basin at the updrift boundary through 40 flow channels, each controlled by its own undershoot weir, with a matching set of flow channels at the downdrift end of the facility. All of the flow channels are 0.5 m in width and the fixed-bed beach has a slope of 1:20. This system allows the wave-driven LSC to be externally recirculated to establish longshore uniformity of waves and wave-driven currents. Some technical specifications on the facility were found in HR Wallingford (1994).

3. PHYSICAL DESCRIPTION OF THE NEW LABORATORY FACILITY

The LSTF occupies a 30-m cross-shore by 50-m longshore by 1.4 m deep wave basin (Figure 1). Monochromatic and random waves can be generated with four digitally controlled, piston-type, servo-electric wave generators. The wave generators are synchronized to create unidirectional long-crested waves up to 0.5 m in height for wave periods up to 3.0 s, and can be oriented at various angles ranging from 0 to 20 deg with respect to shore normal. For oblique angles of wave attack, the wave generators are phase-shifted to maximize the cross-shore dimension of the testing area. End-baffles, located between two adjacent wave boards, are used to guide the waves and prevent the formation of spurious waves caused from wave diffraction from the ends of each wave board and from wave energy reflected from the wave absorber located behind the wave generators. Wave guides that follow the refracted wave ray will be designed to facilitate current and sediment input and output at the lateral boundaries of the beach. Wave, current, and bathymetric data will be collected using a suite of sensors located on a custom-designed instrumentation bridge, as described by Rosati et al. (1995).

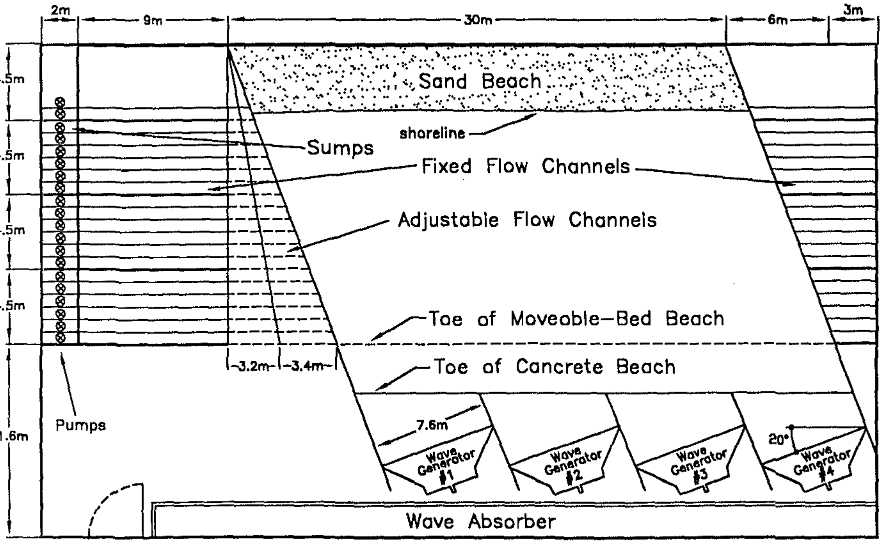

Figure 1: Plan View of the Longshore Sediment Transport Facility

The fixed-bed (concrete) beach has a longshore dimension of 30 m and a cross-shore dimension of 21 m, and was accurately constructed (tolerance of ± 2.0 mm) with parallel contours. The main section of the concrete beach has a constant slope of 1:30, and the toe of the beach slopes down to the basin floor at a slope of 1:18. During future LST experiments, a 0.3 m thick moveable-bed of quartz sand will be placed on top of the fixed-bed beach and will extend 18.0 m offshore (see toe of moveable-bed beach in Figure 1). The toe of the beach will taper down to the basin floor at a slope of 1:6.5.

A LSC recirculation system is being designed to minimize the adverse laboratory effects resulting from the updrift and downdrift boundaries, and to maximize the length of beach over which longshore uniformity of waves and wave-driven currents exist in the facility. A LSC recirculation system creates a closed-loop system that continuously recirculates LSC from the downdrift to the updrift lateral boundary of the beach, while waves are being generated. As shown in Figure 1, the LSC recirculation system will extend 18.0 m offshore corresponding to the offshore limit of the moveable-bed beach which will be constructed for future LST experiments. A series of pumps will be located at the downdrift end of the facility and will recirculate the wave-driven LSC back to the updrift end of the facility through a series of pipes.

4. NUMERICAL SIMULATIONS OF LSC

The first part of this section provides a description of the numerical model used to estimate the magnitude and cross-shore distribution of the longshore current that will be generated in the LSTF. Subsequent sections describe the setup of the numerical model, validate the results obtained from the numerical model with dye measurements in the LSTF, and show the influence of wave height, period and direction on the estimated magnitude and cross-shore distribution of the longshore current.

4.1 Description of the Numerical Model

Kraus and Larson's (1991) numerical model NMLONG (Numerical Model of the LONGshore current) was used to estimate the wave-driven longshore current in the LSTF. NMLONG is a PC-based model that calculates wave transformation, mean water surface elevation, and longshore current for a 1-D cross-section of beach. The major assumptions in NMLONG are longshore homogeneity and linear wave theory.

Wave transformation in NMLONG includes shoaling, refraction, breaking with energy dissipation, and wave reformation. Random wave transformation is simulated by assuming a Rayleigh distribution of wave heights offshore (waves are assumed to be narrow banded in frequency and direction, so randomness enters only in variability in wave height). NMLONG randomly selects wave heights from the Rayleigh distribution and transforms them as individual waves. The individual wave heights are used to calculate root-mean-square wave height at each point across the profile. This approach neglects wave-wave interactions. The mean water surface elevation (setup and setdown) produced by waves is calculated from the cross-shore momentum balance. The wave forcing (radiation stress) is calculated from linear wave theory.

Wave-driven longshore current is calculated from the longshore momentum balance. The model includes wave forcing (gradients in radiation stress), lateral mixing, and bottom friction. Lateral mixing is modeled with an eddy viscosity approach. Bottom friction is nonlinear (in the unknown current velocity) and requires time-averaging of nonlinear terms over the wave period. The offshore boundary condition for the current is zero wave-driven velocity. For random wave simulation, longshore currents from individual waves are averaged at each profile point.

Using the data from Visser (1982), Kraus and Larson (1991) illustrated that NMLONG can be calibrated to reproduce the LSC measured in the laboratory with reasonable success. In particular, the magnitude and cross-shore location of the peak of the LSC distribution was reproduced with reasonable accuracy. This suggests that NMLONG can be used to provide a reasonable estimate of the magnitude and cross-shore distribution of LSC that can be generated in the LSTF. However, in the Visser cases, NMLONG predicted that the magnitude of the offshore tail of the LSC distribution was higher than measured by Visser, even after the numerical model had been calibrated.

4.2 Numerical Model Setup

NMLONG requires the following input parameters: offshore wave height, period, and direction, specification of regular or random waves, offshore water depth, and beach profile elevation relative to mean water level. Random waves are characterized in NMLONG using the root-mean-square wave height, H_{rms}. Values of H_{rms} were converted to significant wave height, H_s assuming $H_s = 1.414 \times H_{rms}$. Nonlinear bottom friction with a friction coefficient equal to 0.01 was used in the LSTF simulations. For one wave condition, the sensitivity of results to this value was evaluated by reducing and increasing the coefficient to 0.005 and 0.02, respectively. All other empirical parameters were set to the default values: incipient breaking-wave-height-to-water-depth-ratio equal to 0.8, stable wave-height-to-water-depth-ratio equal to 0.4, energy flux dissipation rate equal to 0.15, and lateral mixing coefficient equal to 0.3.

NMLONG was set up to calculate the depth-averaged LSC velocities at each cell spaced 1 m across the beach profile. These depth-averaged velocities were multiplied by the corresponding mean water depth and integrated across the entire profile to estimate the total longshore volume flux for each wave condition.

Two series of numerical simulations were conducted to represent two different experimental configurations planned for the LSTF. The first series was conducted with an offshore water depth equal to 0.6 m and represents the configuration that will be used in the LSTF during the hydrodynamic testing phase. The second series was conducted with a water depth equal to 0.9 m and represents the configuration that will be used for the moveable-bed LST experiments. In this configuration a 0.3 m thick uniform layer of sand will be placed on top of the existing concrete beach. Increasing the water level from 0.6 to 0.9 m translates the shoreline directly upwards (i.e., there is no cross-shore translation of the nearshore zone). However, the resulting magnitude and cross-shore distribution of the LSC is slightly different for the two different configurations, due to the slight difference in wave transformation caused by the steeper toe of the beach in the case with the moveable-bed.

Numerical simulations in both test series covered the following range of hydrodynamic conditions: significant wave height, H_s = 0.1 to 0.4 m, peak wave period, T_p = 1.0 to 2.5 s, and angle of wave incidence, θ = 5 to 20 deg relative to shore normal. For these test conditions total longshore volume flux ranged from 0.04 m^3/s for H_s = 0.1 m, T_p = 2.5 s, and θ = 20 deg to 1.3 m^3/s for H_s = 0.4 m, T_p = 2.5 s, and θ = 20 deg.

The sensitivity of the bottom friction coefficient was evaluated for a relatively energetic wave condition; namely H_s = 0.3 m, T_p = 2.5 s and θ = 20 deg. The bottom friction coefficient was varied over a range of two times the default value of 0.01 (i.e., from 0.005 to 0.02). Results obtained using the lower friction coefficient (0.005) resulted in a total longshore volume flux of 1.1 and 1.2 m^3/s for the 0.6 and 0.9 m water depth cases, respectively. The higher friction coefficient (0.02) reduced the total longshore volume flux to 0.4 m^3/s for both water depth cases. Therefore, the results obtained using NMLONG to predict the total longshore volume flux in the LSTF are sensitive to the value of the bottom friction coefficient.

4.3 Validation with Dye Measurements in the LSTF

Preliminary estimates of the magnitude of the LSC were obtained in the LSTF by injecting dye into the surf zone while generating monochromatic waves. These measurements were then used to assess the validity of the numerical simulations. However, the following facility components had not been installed in the LSTF at the time these measurements were required: (1) lateral wave guides were not available to train the incident waves from the wave generators to the surf zone, (2) none of the LSC recirculation system components were available to minimize the laboratory effects caused by the lateral boundaries of the facility (i.e., pumps and flow channels), and (3) only monochromatic waves could be generated with the wave makers, As a result, strong adverse reflection patterns (from the vertical walls at the two ends of the basin) and circulation cells developed throughout the facility as the first 5-10 waves were generated. In addition, no flow velocity measurement sensors were available to accurately measure the wave driven LSC in the surf zone.

Three conclusions were made based on these limited dye measurements. First, NMLONG produced reasonable estimates of the peak LSC magnitude and cross-shore location, using the default bottom friction coefficient of 0.01. However, insufficient data were collected to calibrate this coefficient. Secondly, we were unable to verify the cross-shore distribution of the LSC predicted using NMLONG due to the physical limitations and resulting adverse laboratory effects discussed above. Therefore, the default lateral mixing coefficient (0.30) was used. Thirdly, observations made while these dye measurements were being carried out strongly reinforced the expectation that a properly designed external LSC recirculation system would be required to maintain longshore uniformity of waves and wave-driven currents in the facility, especially for energetic wave conditions.

4.4 Influence of Hydrodynamic Variables

The influence of wave height, period and direction on the magnitude and cross-shore distribution of the LSC was investigated. All numerical simulations were conducted using random waves. Figure 2 shows the LSC distribution for H_s = 0.2, 0.3, and 0.4 m, with T_p = 2.5 s and θ = 20 deg at the wave generator. Three general trends can be seen in this figure. First, as H_s increases, the magnitude of the LSC at the peak of the distribution significantly increases. The magnitude of the peak LSC equals 0.21, 0.28 and 0.36 m/s for H_s = 0.2, 0.3 and 0.4 m, respectively. This is a relative increase of approximately 30% for each 0.1 m increase in wave height. Secondly, the peak of the LSC distribution moves offshore as H_s increases, because the incident waves begin to break further offshore. Thirdly, the width of the LSC distribution increases as the H_s increases, since the width of the surf zone increases.

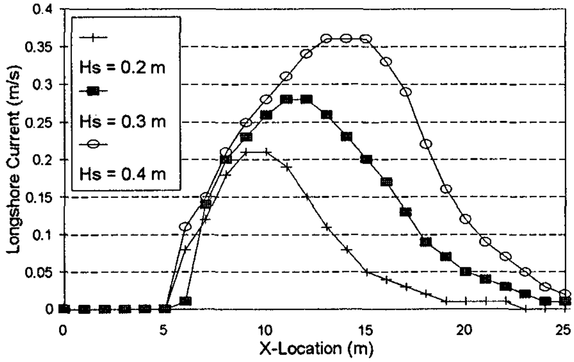

Figure 2: Influence of Significant Wave Height

Figure 3 shows the LSC distribution for T_p = 1.0, 1.5, 2.0 and 2.5 s with H_s = 0.3 m and θ = 20 deg at the wave generator. Three general trends can be seen in this figure. First, as T_p increases, the magnitude of the LSC at the peak of the distribution increases slightly. The magnitude of the peak LSC equals 0.25, 0.26, 0.27 and 0.28 m/s for T_p = 1.0, 1.5, 2.0 and 2.5 s, respectively. This is a relative increase of only 4% for each 0.5 s increase in T_p. Secondly, the peak of the LSC distribution moves slightly further offshore as T_p increases, since the incident waves begin to break slightly further offshore. Thirdly, the width of the LSC distribution increases slightly as T_p increases, since the width of the surf-zone increases slightly.

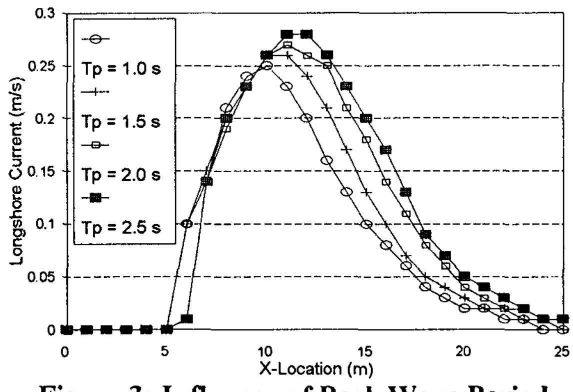

Figure 3: Influence of Peak Wave Period

Figure 4 shows the LSC distribution for θ = 5, 10, 15 and 20 deg with H_s = 0.3 m and T_p = 2.5 s. Three general trends can be seen in this figure. First, as θ increases, the magnitude of the LSC at the peak of the distribution significantly increases. The magnitude of the peak LSC equals 0.10, 0.18, 0.23 and 0.28 m/s for θ = 5, 10, 15 and 20 deg, respectively. This is a relative increase of about 80%, 28%, and 22%, for each consecutive increase in θ. Secondly, the cross-shore location of the peak of the LSC distribution remains constant as θ increases. Thirdly, the width of the LSC distribution remains reasonably constant as θ increases.

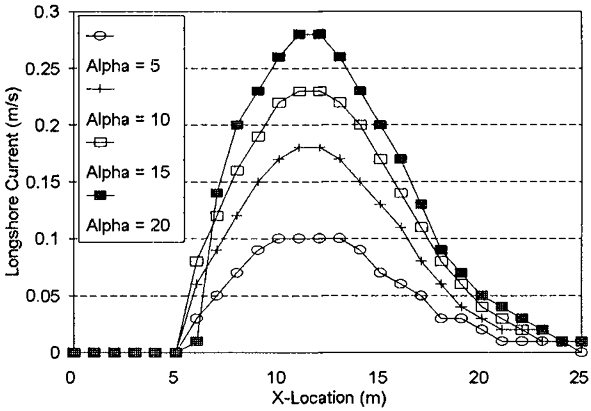

Figure 4: Influence of Incident Wave Direction

In summary, increasing H_s has a strong influence on increasing the magnitude and cross-shore location of the peak of the LSC distribution, whereas, increasing T_p has a much milder effect. Increasing θ has a very strong influence on increasing the peak magnitude, but no influence on the cross-shore location of the peak of the LSC distribution.

5. DESIGN PARAMETERS FOR THE LSC RECIRCULATION SYSTEM

The first part of this section describes the design wave condition used to determine the required pumping capacity of the LSC recirculation system. Subsequent sections discuss a factor of safety applied to the numerical modeling results, and incorporate the requirements of a moveable-bed beach and a variable operating water level into the design.

5.1 Design Wave Condition

To determine the design capacity of a LSC recirculation for the LSTF, a maximum design wave condition was selected. After observing the location of the break point for a number of different wave height and period combinations in the LSTF (and comparing these results with the numerical simulations), it was decided that H_s = 0.3 m and T_p = 2.5 s is probably the most energetic wave condition that will be generated during the moveable-bed LST experiments. As mentioned previously, the maximum angle of wave incidence (measured at the wave generators) to be tested in the LSTF is 20 deg. Therefore, the "design wave condition" used to determine the maximum required pumping capacity of the LSC recirculation system was characterized by $H_s = 0.30$ m, $T_p = 2.5$ s and $\theta = 20$ deg with an offshore water depth of 0.9 m. This is the LSC distribution shown previously in Figure 2 (middle curve) and Figure 3 and 4 (upper curve). Results obtained using NMLONG to predict the magnitude and cross-shore distribution of LSC for this "design wave condition" indicated a total longshore flux of 0.76 m^3/s within the surf zone.

5.2 Determining a Factor of Safety

A factor of safety was incorporated into the design to compensate for inaccuracies in calculating the magnitude and cross-shore distribution of LSC that will be generated in the LSTF. Our concerns included: (1) having inadequate data to calibrate the bottom friction coefficient and the lateral mixing coefficient in the numerical model, and (2) changes in the bottom roughness between the initial hydrodynamic tests on a fixed-bed concrete beach and multiple grain sizes used for the moveable-bed beach for the LST experiments. The surface of the concrete beach was broom-finished to simulate the roughness of a course grained sand. However, because bed-forms will develop in the LST experiments it is likely that the moveable-bed beach will have a higher friction coefficient for a given wave condition. Due to these uncertainties, the magnitude of the LSC at each cross-shore location was increased by 10% (i.e., a Factor of Safety = 1.1) for the purpose of determining the required pumping capacity of the LSC recirculation system.

5.3 Allowance for Maximum Depth of Erosion of the Moveable-Bed Beach

At this point in the design process, predictions of the LSC magnitude and cross-shore distribution to be generated in the LSTF are based on a 1:30 plane sloping fixed-bed beach having parallel contours. However, for future moveable-bed experiments in the LSTF, the beach profile will respond to incident wave conditions, creating a shore-parallel bar and trough feature near the location of initial wave breaking. Assuming longshore uniformity in the beach bathymetry, the capacity of the LSC recirculation system must be increased wherever the beach profile erodes, due to the increased longshore flux at the cross-shore location. For example, in the trough located shoreward of the offshore bar.

To investigate this problem, 2-D flume tests were conducted to estimate the maximum depth of erosion during future moveable-bed LST experiments in the LSTF. Each test started with a 1:30 plane sloping sand beach, with $D_{50} = 0.11$ mm. This is the same initial beach slope and sediment size to be used for the fine-grained sediment test series in the LSTF. In each experiment, the maximum depth of erosion was located just offshore of the still-water shoreline. For the design wave condition the maximum depth of erosion did not exceed 0.1 m, however, this conclusion is based on 2-D flume tests, and not 3-D tests in the LSTF.

For design purposes, it was assumed that the entire 18-m width of the moveable-bed beach will erode by 0.1 m. This is a fairly crude assumption, although it is conservative in that it allows for the maximum scour depth to occur at any location across the beach profile. In particular, this is a very conservative assumption near the offshore end of the beach where accretion should occur (as opposed to erosion) as the offshore bar develops. However, future plans for the LSTF include a test with a terminal groyne located at the downdrift end of the moveable-bed beach. If this physical model behaves as expected, a scour hole will develop at the head of the groyne and the longshore flux (shoreward of the offshore end of the groyne) will be deflected offshore and bypass the end of the groyne. Therefore, over designing the LSC recirculation system near the offshore region of the beach will give the system more flexibility in the future when conducting experiments with coastal structures.

Note that this analysis assumes that the depth-averaged LSC at any cross-shore location does not change substantially (from the case with a plane sloping fixed-bed beach) as the offshore bar and trough feature develop in the moveable-bed experiments. Although this may not be the case, we feel that changes to the depth-averaged LSC (as the beach profile develops) will be relatively small since the initial beach slope is relatively gentle (1:30) and the total profile adjustment should be relatively small. Therefore, this assumption should be adequate for design purposes.

5.4 Allowance for Variable Operating Water Levels in the Facility

The design of the LSC recirculation system also accounted for the requirement to conduct experiments with variable water levels in the facility. As mentioned previously, we plan to conduct the majority of the moveable-bed LST experiments with an offshore water depth of 0.9 m. However, if we decide to increase the water level in the future, the LSC distribution will be translated shoreward on the beach.

A number of physical constraints in the vertical dimension of the facility dictate that the maximum operating water level in the facility will not exceed 1.0 m (at least for energetic wave conditions). Lower water levels can be used, however, the wave generation capability of the wave makers will decrease with decreasing water level. Therefore, the critical design parameter is the maximum operating water level in the facility. The first curve in Figure 5 shows the longshore flux distribution for the design wave condition, with an offshore water depth of 0.9 m. This curve includes the increased capacity required by using a factor of safety of 1.1 and assuming the moveable-bed erodes 0.1 m across the entire width of the beach. The abrupt change in cross-shore gradient at X = 18 and 21 m is caused by the sudden change in beach slope at these locations. The second curve was obtained by increasing the offshore water depth to 1.0 m, for the same design wave condition. Essentially, this 0.1 m increase in operating water level translates the LSC distribution 3.0 m shoreward, because the slope of the concrete beach is 1:30. The third curve in the figure encompasses both the first and second curve, and represents the required pumping capacity of the LSC recirculation system for water levels ranging from 0.9 to 1.0 m. As shown in the figure, incorporating a variable water level into the design essentially broadens the width of the LSC distribution that needs to be recirculated within the facility.

6. OTHER DESIGN CONSIDERATIONS

The following sections describe uncertainties related to how far the LSC distribution extends offshore, the magnitude of the longshore flux of water flowing in the swash zone, and the issue of what percentage of the wave-driven LSC needs to be recirculated.

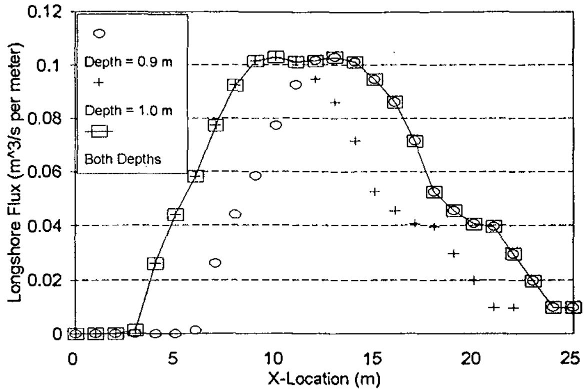

Figure 5: Influence of Offshore Water Depth

6.1 Offshore Tail of the LSC Distribution

Another design consideration is the possibility that a small longshore flux may exist offshore of the toe of the moveable-bed beach (X > 18.0 m), for very energetic wave conditions. Approximately 17% of the area under the curve in Figure 5 is offshore of X = 18 m, which is the location of the offshore end of the recirculation system, as shown in Figure 1. In Section 4.1, it was discussed that NMLONG may over predict how far the LSC distribution extends offshore. Unfortunately, this was impossible to verify due to problems encountered making dye measurements in the partially constructed LSTF, as discussed in Section 4.3. If the numerical simulations are correct, this offshore tail of the LSC distribution may cause adverse internal circulation patterns within the facility.

If this problem exists in the future, there are a number of possible solutions. First, we could decrease the magnitude of the maximum wave condition that is generated in the facility. Second, we could increase the offshore water depth to 1.0 m for very energetic wave conditions, which would shift the LSC distribution 3.0 m shoreward. The area under the curve (offshore of X = 18 m) associated with an offshore water depth of 1.0 m, is only 9% of the total area. Third, it may be possible to oversize the furthest offshore pump, and use the additional capacity to recirculate some of the LSC which exists offshore of X = 18 m. Based on these considerations, it was decided that the LSC recirculation system would initially be constructed to extend offshore to X = 18.0 m. If the numerical predictions turn out to be correct, one or more of the options discussed above will be employed.

6.2 Longshore Flux of Water in the Swash Zone

Another design feature to be considered is the longshore flux of water flowing downdrift within the swash zone. The swash zone was defined as the area between the still-water shoreline and the maximum point of wave uprush, including any setup in the mean water level. Unfortunately, it is impossible to accurately calculate the longshore flux in the swash zone due to our limited understanding of swash zone processes. One of the interesting results obtained from the 2-D moveable-bed tests, discussed previously in Section 5.3, is that the swash zone was approximately 4 m in width for the design wave condition. Therefore, it is believed that it will be necessary to recirculate the longshore flux in the swash zone, due to the physical size of the swash zone that develops at this relatively large geometric scale.

Figure 5 indicates that at X = 5.0 m, the longshore flux of water will be approximately 0.045 m^3/s per meter width of beach. In addition, we know that the longshore flux of water at the landward boundary of the swash zone will be zero. Therefore, we can make a somewhat crude assumption and draw a straight line between these two points to represent the time-averaged longshore flux of water flowing downdrift in the swash zone. Although we expect the longshore flux of water to have a nonlinear distribution across the swash zone, this assumption provides a first-order estimate for design purposes.

6.3 Percentage of Longshore Flux to be Externally Recirculated

Intuitively one would expect that 100% of the longshore flux within the surf zone should be externally recirculated back to the updrift end of the facility with a LSC recirculation system. However, laboratory facilities are not ideal systems and in many cases an internal circulation pattern may exist, in which case it may not be necessary (or possible) to externally recirculate 100% of the wave-driven longshore flux without adding too much momentum into the system. Visser (1982) developed a method to obtain a uniform LSC distribution along the finite length of a straight beach in a 3-D wave basin. Visser determined the "proper" rate of external recirculation by adjusting the pumping rate and inflow distribution until the internal circulation between the wave guides was minimized. However, after reviewing Visser's work, Svendsen (1991) concluded that in some of Visser's experiments the internal circulation was still disturbingly large (as much as 40-50% of the wave-driven longshore flux within the surf zone), even though Visser's data indicate that he was able to establish a LSC distribution that was relatively uniform alongshore.

Based on Svendsen's conclusion and the principle of continuity, Visser's external recirculation flow rate must have been substantially less than the total longshore flux in the surf zone. This indicates that it may not be necessary to recirculate 100% of the longshore flux in the LSTF, to obtain longshore uniformity. This problem will be investigated in the LSTF during the initial hydrodynamic experiments on a fixed-bed beach. However, for the purpose of estimating the required pumping capacity of the LSC recirculation system, it was prudent to assume that 100% of the longshore flux will need to be externally recirculated.

7. DESIGN CAPACITY FOR EACH INDIVIDUAL PUMP

The last step in this phase of the design process was to determine the design capacity of each of the individual pumps that make up the LSC recirculation system. Required pump capacity is a function of the width of the flow channels at the downdrift end of the facility, which is directly related to the cross-shore resolution of the LSC recirculation system. Intuitively, one would expect that the higher the cross-shore resolution, the longer the "working beach region" where longshore uniformity of waves and wave-driven LSC's exist. After reviewing the design of LSC recirculation systems used in other laboratory facilities (see Section 2) it was decided that the flow channels at the downdrift and updrift end of the LSTF should be 0.75 m in width. This was a compromise between cross-shore resolution and the estimated cost of construction of the entire LSC recirculation system.

Knowing the required pumping capacity of the LSC recirculation system, shown in Figure 5 (third curve), and given a flow channel width of 0.75 m, the capacity of each individual pump could be readily calculated. Figure 6 shows a bar graph expressed in m^3/s for every 0.75 m of beach width, and the magnitude of each bar represents the required pumping capacity of each individual pump. This figure also includes the required pumping capacity to recirculate the longshore flux in the swash zone (see Section 6.2). Figure 6 shows 23 pump capacities. However, to reduce the number of pumps near the shoreline, where the longshore flux is relatively small, one large pump will be used as opposed to four smaller pumps, as illustrate in Figure 1. Therefore, there will be a total of 20 pumps in the system.

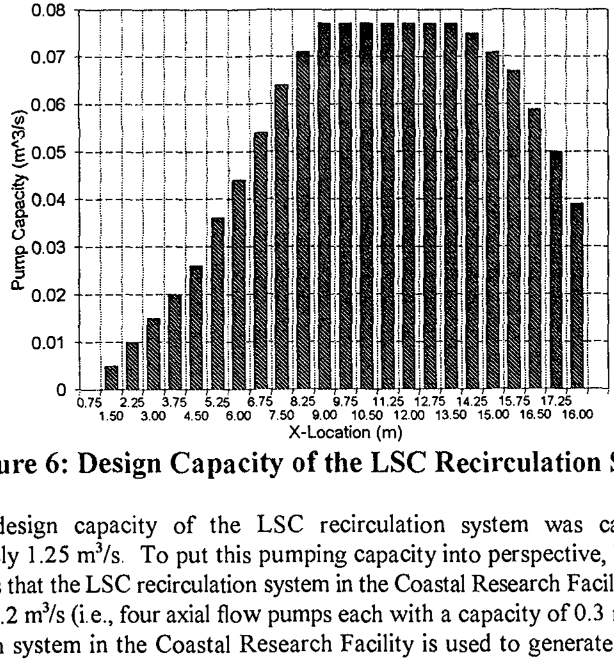

Figure 6: Design Capacity of the LSC Recirculation System

The total design capacity of the LSC recirculation system was calculated to be approximately 1.25 m^3/s. To put this pumping capacity into perspective, HR Wallingford (1994) states that the LSC recirculation system in the Coastal Research Facility has a design capacity of 1.2 m^3/s (i.e., four axial flow pumps each with a capacity of 0.3 m^3/s). The LSC recirculation system in the Coastal Research Facility is used to generate not only wave-driven LSC within the surf zone, but also tidal currents offshore of the toe of the concrete beach. Therefore, although the purpose of the two systems in not exactly the same, the total design pumping capacities are very similar.

8. SUMMARY

This paper documents the design process used to determine the required pumping capacity of an external longshore current recirculation system for the development of a longshore sediment transport laboratory facility. A design wave condition of $H_s = 0.3$ m, $T_p = 2.5$ s, and $\theta = 20$ deg, with an offshore water depth of 0.9 m was used to estimate the magnitude and cross-shore distribution of the longshore current that will be generated in the new facility. By including a factor of safety and considering a number of functional design requirements, the total required design pumping capacity was determined to be 1.25 m^3/s. It was estimated that twenty independent pumps and flow channels would be required to provide adequate cross-shore resolution for the system and to provide the required capability to recirculate a broad range of LSC distributions for a wide range of incident wave conditions, water levels and moveable-bed beach profiles.

9. ACKNOWLEDGEMENTS

The authors would like to thank the staff at HR Wallingford, in the United Kingdom for generously providing technical information about the Coastal Research Facility. This paper benefited from the review comments of Bruce A. Ebersole. This research is funded by the "Large-Scale Laboratory Investigation of Longshore Sediment Transport" work unit of the Coastal Sediment and Dredging Program, under the Coastal Navigation and Flood Damage Reduction Research Area. Permission to publish this paper was granted by the Chief of Engineers, U.S. Army Corps of Engineers.

10. REFERENCES

Brebner, A., and Kamphuis, J.W. 1963. Model Tests on the Relationship Between Deep-Water Wave Characteristics and Longshore Currents. Report No. 31, Department of Civil Engineering, Queen's University at Kingston, Canada.

Galvin, C.J., and Eagleson, P.S. 1965. Experimental Study of Longshore Currents on a Plane Beach. Technical Memorandum No. 10, US Army Waterways Experiment Station, Coastal Engineering Research Center, Vicksburg, MS, USA.

HR Wallingford (1994). Understanding the Nearshore Environment. A publication describing the Coastal Research Facility at HR Wallingford, 4 p.

Kraus, N.C., and Larson, M. 1991. NMLONG: Numerical Model for Simulating the Longshore Current, Report 1: Model Development and Tests. Technical Report DRP-91-1, US Army Engineer Waterways Experiment Stations, Vicksburg, MS.

Mizuguchi, M. And Horikawa, K. 1978. Experimental Study on Longshore Current Velocity Distribution, Bulletin 21, pp 123-150, Facul. Sci. & Eng., Chuo University.

Putnam, J.A., Munk, W.H., and Taylor, M.A., 1949. The Prediction of Longshore Currents. Transactions of the American Geophysical Union, Vol. 30 (3), pp 337- 345.

Rosati, J.D., Hamilton, D.G., Fowler, J.E. and Smith, J.M. 1995. Design of a Laboratory Facility for Longshore Sediment Transport Research. Proc. of Coastal Dynamics '95, pp 771-782, Gdansk, Poland.

Shore Protection Manual 1984. USACE Waterways Experiment Station, Coastal Engineering Research Center, Vicksburg, MS, 2 Vols.

Simons, R.R., Whitehouse, R. JS., MacIver, R.D., Pearson, J., Sayers, P.B., Zhao, Y., and Channell, A.R. 1995. Evaluation of the UK Coastal Research Facility. Proc. of Coastal Dynamics '95, pp 161-172, Gdansk, Poland.

Svendsen, I.A. 1991. Development of a Comprehensive Plan for Modeling Longshore Current Generation in the Laboratory. Unpublished Contract Report for the Waterways Experiment Station, Coastal Engineering Research Center, Vicksburg, MS.

Visser, P.J. 1982. The Proper Longshore Current in a Wave Basin. Report No. 82-1, Department of Civil Engineering, Delft University of Technology, The Netherlands.